Na leak with gating pore properties in hypokalemic periodic paralysis V876E mutant muscle Ca channel

Clarisse Fuster,[1] Jimmy Perrot,[1] Christine Berthier,[1] Vincent Jacquemond,[1] Pierre Charnet,[2] and Bruno Allard[1]

[1]Institut NeuroMyoGene, Université Lyon 1, Université de Lyon, UMR Centre National de la Recherche Scientifique 5310, Institut National de la Santé et de la Recherche Médicale U1217, Villeurbanne, France
[2]Institut des Biomolécules Max Mousseron, Université Montpellier 1 et 2, UMR Centre National de la Recherche Scientifique 5247, Montpellier, France

Type 1 hypokalemic periodic paralysis (HypoPP1) is a poorly understood genetic neuromuscular disease characterized by episodic attacks of paralysis associated with low blood K^+. The vast majority of HypoPP1 mutations involve the replacement of an arginine by a neutral residue in one of the S4 segments of the α1 subunit of the skeletal muscle voltage-gated Ca^{2+} channel, which is thought to generate a pathogenic gating pore current. The V876E HypoPP1 mutation has the peculiarity of being located in the S3 segment of domain III, rather than an S4 segment, raising the question of whether such a mutation induces a gating pore current. Here we successfully transfer cDNAs encoding GFP-tagged human wild-type (WT) and V876E HypoPP1 mutant α1 subunits into mouse muscles by electroporation. The expression profile of these WT and V876E channels shows a regular striated pattern, indicative of their localization in the t-tubule membrane. In addition, L-type Ca^{2+} current properties are the same in V876E and WT fibers. However, in the presence of an external solution containing low-Cl^- and lacking Na^+ and K^+, V876E fibers display an elevated leak current at negative voltages that is increased by external acidification to a higher extent in V876E fibers, suggesting that the leak current is carried by H^+ ions. However, in the presence of Tyrode's solution, the rate of change in intracellular pH produced by external acidification was not significantly different in V876E and WT fibers. Simultaneous measurement of intracellular Na^+ and current in response to Na^+ readmission in the external solution reveals a rate of Na^+ influx associated with an inward current, which are both significantly larger in V876E fibers. These data suggest that the V876E mutation generates a gating pore current that carries strong resting Na^+ inward currents in physiological conditions that are likely responsible for the severe HypoPP1 symptoms associated with this mutation.

INTRODUCTION

Propagation of action potentials along the muscle cell membrane induces Ca^{2+} release from the SR and subsequent contraction of the cell. In the sequence of events that occur from excitation to contraction, the Cav1.1 protein anchored in the t-tubule membrane plays the dual role of voltage sensor of SR Ca^{2+} release and of L-type voltage-gated Ca^{2+} channel (Ríos and Pizarro, 1991; Schneider, 1994; Melzer et al., 1995). Given these pivotal roles, the absence of Cav1.1 is lethal, and any mutation occurring in the gene encoding Cav1.1 and producing changes in the functional properties of the protein leads to severe neuromuscular diseases. Among them, type 1 hypokalemic periodic paralysis (HypoPP1) is one of the least understood genetic disorders, characterized by transient failure of muscle excitability occurring in association with hypokalemia and triggered by rest after strenuous exercise or carbohydrate load (Lehmann-Horn et al., 2004; Cannon, 2015). Cav1.1 is composed of 4 homologous domains (I to IV), each of which contains 6 membrane-spanning segments (S1 to S6; Catterall, 2011). S1 to S4 segments of each domain constitute the voltage-sensing domain, within which S4 segments enriched with positively charged amino acids are able to translocate through a "gating pore" pathway formed by the S1, S2, and S3 segments upon depolarization (Gandhi and Isacoff, 2002). This concerted translocation of the S4 segments controls the gating of the L-type Ca^{2+} channel and Ca^{2+} release from the SR. The vast majority of HypoPP1 mutations identified so far were shown to consist in the replacement of the outermost arginine residues by less basic residues in S4 segments of domains II, III, or IV (Cannon, 2010; Matthews and Hanna, 2010; Jurkat-Rott et al., 2012; Moreau et al., 2014). Site-directed mutagenesis experiments in the closely structurally related voltage-dependent K^+ or Na^+ channels have revealed that such substitutions generated an inward gating pore current at hyperpolarized potentials, also called the ω current, through the voltage-sensing domain (Starace and Bezanilla, 2004; Sokolov et al., 2005; Tombola et al., 2005). In addition, experiments performed in fibers from muscle biopsies

Correspondence to Bruno Allard: bruno.allard@univ-lyon1.fr
Abbreviations used: HypoPP1, type 1 hypokalemic periodic paralysis; pHi, intracellular pH; SBFI, sodium-binding benzofuran isophthalate.

The Rockefeller University Press
J. Gen. Physiol. 2017 Vol. 149 No. 12 1139–1148
https://doi.org/10.1085/jgp.201711834

in patients carrying HypoPP1 mutations and in muscle fibers from a transgenic mouse model for HypoPP1 indicated that the R528H or the R1239H mutation gave rise to an elevated inward current at resting membrane potentials which, in the presence of severely decreased serum K^+ concentrations, should depolarize muscle cells so as to inactivate voltage-dependent Na^+ channels and induce attacks of paralysis (Jurkat-Rott et al., 2009; Wu et al., 2012). The ion carried by this leak current was not determined, but mutagenesis experiments performed in voltage-dependent K^+ or Na^+ channels showed that the inward current flowing through the gating pore at hyperpolarized potentials was carried by protons when the outermost arginine residues in S4 segments were replaced by histidine residues (Starace and Bezanilla, 2004; Struyk and Cannon, 2007). More recently, by expressing the human WT and R1239H mutant α1 subunits in mouse muscle fibers, Fuster et al. (2017) demonstrated that the R1239H mutation induces an elevated leak H^+ current at rest flowing through a gating pore created by the mutation in the voltage-dependent Ca^{2+} channel. Strikingly, one more recently identified HypoPP1 mutation, V876E, which produces very severe clinical features, does not affect an arginine residue in a S4 segment but occurs in the S3 segment of domain III (Ke et al., 2009). This raises the question if in such a case the mutation induces a gating pore current and, if so, about the ion selectivity of this gating pore pathway.

In the present study, we have been able to acutely express in adult mouse muscles human WT and V876E Cav1.1 proteins. Measurements of membrane currents indicate that the mutation does not induce any significant change in properties of the voltage-gated Ca^{2+} current but generates an elevated leak inward current at negative voltages. In the absence of external permeant ions and with low chloride, the leak current was found to be carried by H^+, but in the presence of a physiological external saline, measurement of intracellular pH and Na^+ together with membrane currents indicated that the leak current in V876E fibers is carried by Na^+. Our data suggest that the valine residue, when replaced by the negatively charged amino acid glutamate, creates a hydrophilic pathway, possibly corresponding to a gating pore permeable to Na^+ ions.

MATERIALS AND METHODS

In vivo gene transfer and isolation of muscle fibers

All experiments were performed in accordance with the guidelines of the local animal ethics committee of University Lyon 1, of the French Ministry of Agriculture (87/848), and of the European Community (86/609/EEC). Expression was achieved by in vivo plasmid transfer using a previously described electroporation procedure with minor modifications (DiFranco et al., 2006; Fuster et al., 2017). Injected plasmids encoded for turboGFP-tagged WT or V876E human Cav1.1 (Origene). Muscle fiber isolation was performed 30 ± 5 d later. Mice were killed by cervical dislocation before removal of interosseal muscles. Single fibers were isolated by a 50-min enzymatic treatment at 37°C using a Tyrode's solution containing 2 mg/ml collagenase type I (Sigma-Aldrich).

Electrophysiology

Fibers were voltage-clamped using the silicone clamp technique as previously described. In brief, the major part of a single fiber was electrically insulated with silicone grease, and a micropipette was inserted into the fiber through the silicone layer to voltage clamp the portion of the fiber free of grease (50–150 µm length) using a patch-clamp amplifier (RK-400, Bio-Logic) in the whole-cell configuration (Robin and Allard, 2015). Analogue compensation was systematically used to decrease the effective series resistance. The tip of the micropipette was then crushed into the dish bottom to allow intracellular dialysis of the fiber with the intrapipette solution. Cell capacitance was determined by integration of a current trace obtained with a 10-mV hyperpolarizing pulse from the holding potential and was used to calculate the density of currents (A/F). For Ca^{2+} current measurements, leak currents were subtracted from all recordings using the same pulse preceding every test pulse supposing a linear evolution of leak current with depolarization. The voltage dependence of the mean Ca^{2+} current density was fitted using the equation

$$I = G\max(Em - Erev)/(1 + \exp((E_{1/2} - Em)/k)),$$

where I is the mean density of the current measured, Em is the test pulse, Gmax is the maximum conductance, Erev is the apparent reversal potential, $E_{1/2}$ is the half-activation voltage, and k is a steepness factor. Voltage ramps were applied every 50 s at a rate of 12 mV/s throughout the study. Concerning the experiments illustrated in Fig. 4, a holding potential maintained at 0 mV during the 50-s interval between ramps avoided a possible dissipation of the H^+ gradient resulting from proton influx upon exposure of the cell to the pH 6.0 buffered solutions because inward rectification made the inward proton current close to zero at 0 mV. Currents were acquired at a sampling frequency of 10 kHz.

Measurement of intracellular pH (pHi) and intracellular Na^+

The pHi indicator 2',7'-bis-(2-carboxyethyl)-5-(and-6)-carboxyfluorescein (BCECF; ThermoFisher Scientific) was added at 100 µM in the internal pipette solution. The pH-dependent signal was obtained by alternatively illuminating the cell at 490 and 440 nm through an optical fiber using a monochromator (Cairn Research) and imaging fluorescence >510 nm using a 40× oil-immer-

sion objective and a CoolSNAP$_{EZ}$ charge-coupled device camera (Roper Scientific). Background fluorescence at both excitation wavelengths was measured from an equivalent area next to each fiber tested and subtracted, and the ratio F490/F440 was calculated. The frequency of image capture was 0.2 Hz. For the conversion of fluorescence ratios into pHi, each fiber was exposed at the end of the experiments to solutions buffered at pH 5.5, 7, and 8 in the presence of the H^+ ionophore nigericin. The 3 measured fluorescence ratios were converted into pH values by fitting the relationship between these ratios and pHi with the following equation:

$$pHi = pKa + \log[(R - R\,min)/(R\,max - R)],$$

where pKa is the −log dissociation constant, R is the 490/440 ratio measured at pH 5.5, 7, and 8, and Rmin and Rmax are the ratios of the dye in its H^+-free and H^+-bound state, respectively. In Fig. 5 B, because pHi measurements have been done alternatively in WT, R1239H, and V876E fibers during the same period, the WT data points are the same as the ones reported in another study investigating the R1239H mutation (Fuster et al., 2017). For intracellular Na^+ measurements, the Na^+ indicator sodium-binding benzofuran isophthalate (SBFI; ThermoFisher Scientific) was added at 200 µM in the internal pipette solution, and the Na^+-dependent signal was obtained by alternatively illuminating the cell at 340 and 380 nm and imaging fluorescence >510 nm. The rates of change of pHi and SBFI fluorescence ratio were measured by fitting a linear regression to data points. BCECF and SBFI fluorescence changes were observed to be restricted to the voltage-clamped region of the fibers.

Solutions

For Figs. 1, 2, 3, and 4, the external solution contained (in mM) 140 TEA-$MeSO_3$, 2.5 $CaCl_2$, 1 $MgCl_2$, 0.002 tetrodotoxine, 1 4-aminopyridine, and 10 HEPES or Mes adjusted to pH 7.2 or 6 with TEA-OH or $MeSO_3$ acid. For Figs. 5, 6, and 7, the external Tyrode's solution contained (in mM) 140 NaCl or 140 NMDG chloride, 5 KCl, 2.5 $CaCl_2$, 1 $MgCl_2$, and 10 HEPES or Mes adjusted to pH 7.2 or 5 with NaOH or $MeSO_3$ acid. The internal dialyzed solution contained (in mM) 120 K-glutamate, 10 EGTA, 5 Na_2-ATP, 5 Na_2-phosphocreatine, 5.5 $MgCl_2$, 5 glucose, and 10 HEPES adjusted to pH 7.2 with K-OH, except for Figs. 5, 6, and 7, where the internal solution was free of EGTA. For BCECF calibration, fibers were exposed at the end of the experiment to solutions containing (in mM) 140 K-glutamate, 2 $MgCl_2$, 10 HEPES, or Mes adjusted to pH 8, 7, or 5.5 with K-OH or $MeSO_3$ acid in the presence of the H^+ ionophore nigericin (10 µM). Nigericin (Sigma-Aldrich) was used from a stock solution at 10 mM in DMSO. Fibers were dialyzed with the intracellular solution through the micropipette during 20 min prior starting the experiments.

Statistics

Fits were performed with Microcal Origin (Microcal Software Inc.). Data are given as means ± SEM and compared using unpaired two-tailed Student *t* tests (or paired when mentioned). Differences were considered significant when $P < 0.05$. Labels *, **, and *** indicate $P < 0.05$, $P < 0.005$, and $P < 0.0005$, respectively. Current data exhibited quite large variability, certainly because of the variability in the amount of proteins expressed from one fiber to another, which resulted in large values of variance, but did not compromise the revealed statistical differences.

RESULTS

Expression of V876E HypoPP1 mutant Cav1.1 in mouse muscle fibers

cDNAs encoding turboGFP-tagged human WT and V876E HypoPP1 mutant Cav1.1 were transfected by electroporation into adult hind limb mice muscles. Confocal fluorescence images revealed a regular striated pattern of expression perpendicular to the longitudinal axis of the fiber for the two channel types (Fig. 1 A). The fluorescence profile showed periodic double peaks of high intensity with a spacing of ∼2 µm consistent with proper localization of the human WT and V876E channel in the t-tubule membrane (Fig. 1 B). The WT and V876E GFP-positive fibers were selected for voltage clamping. The silicone clamp method allowed focus of the measurements on the highest expressing region of fibers transfected with either the WT or the R1239H Cav1.1 α1 subunit.

Comparison of voltage-gated Ca^{2+} currents properties in fibers expressing WT and V876E Cav1.1

The properties of the L-type voltage-gated Ca^{2+} currents were compared in fibers expressing WT and V876E Cav1.1 by applying depolarizing steps of 1 s duration and increasing amplitudes from a holding potential of −80 mV in the presence of 2.5 mM external Ca^{2+} (Fig. 2). Fitting a Boltzmann equation in each WT and V876E cell indicated that the fitting parameters, maximal conductance, reversal potential, half-maximal activation, and steepness factor were not significantly changed in V876E as compared with the parameters obtained for WT fibers.

Comparison of background currents and resting conductance in WT and V876E fibers

Voltage clamp studies in HypoPP1 R528H fibers from transgenic mice or from human biopsies and in mouse fibers transfected with the HypoPP1 R1239H α1 subunit detected an elevated inward current at hy-

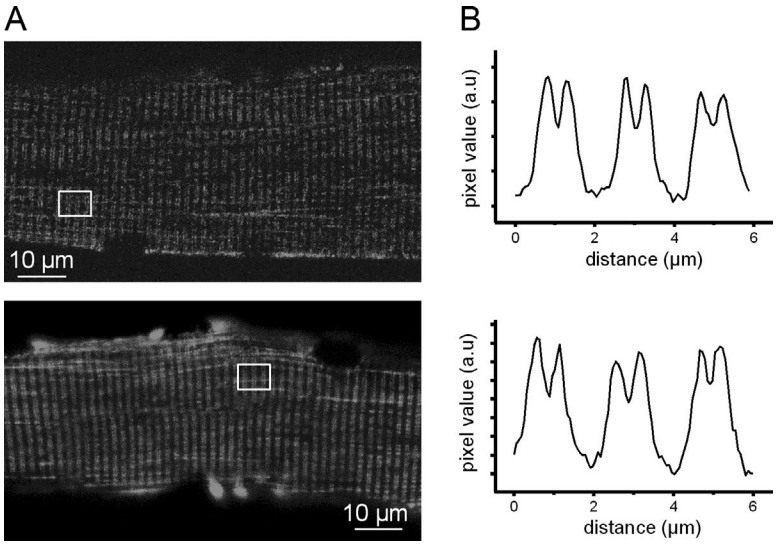

Figure 1. **Distribution of GFP-tagged human WT and V876E Cav1.1 in adult mouse skeletal muscle fibers.** (A) Confocal images of GFP fluorescence in a fiber expressing WT (top) and V876E (bottom) Cav1.1. (B) Fluorescence intensity profiles from the white box region in the corresponding images in A.

perpolarized potentials in mutant fibers (Jurkat-Rott et al., 2009; Wu et al., 2012; Fuster et al., 2017). Considering that the V876E HypoPP1 mutation is associated with comparable clinical features as the R528H mutation, we investigated whether V876E fibers exhibited elevated leak current and conductance by applying hyperpolarizing voltage ramps bringing the internal potential to −120 mV from a starting potential of 0 mV using the same internal and external solutions as those used for voltage-gated Ca^{2+} current recordings. Fig. 3 A shows that membrane currents were more inward in V876E fibers for voltages less negative than −40 mV as compared with WT fibers. Fitting a linear regression between currents and voltages over the −80 to −120 mV range in WT and V876E fibers indicated that the slope conductance was significantly higher in V876E fibers whatever the starting holding potential—0, −20, −40, or −60 mV (Fig. 3 B).

Effects of a change in external pH on background currents and resting conductance in V876E fibers

The preceding series of experiments was performed in the presence of an external solution devoid of Na^+ and K^+ and in low Cl^-, so that the main monovalent cation capable of entering the cell at negative voltages is H^+. Furthermore, a recent study indicated that the HypoPP1 R1239H mutation gave rise to a resting leak current carrying protons (Fuster et al., 2017). To test whether the elevated leak current was carried by H^+ in V876E fibers, we measured the change in membrane currents elicited by hyperpolarizing voltage ramps in response to a change in external pH from 7.2 to 6, which is expected to shift the electrochemical gradient for protons by 70 mV toward positive values. As illustrated in Fig. 4 A, a decrease of external pH from 7.2 to 6 made the background current more inward for voltages lower than −40 mV in a V876E fiber. This effect was also observed in WT fibers. However, subtracting in each

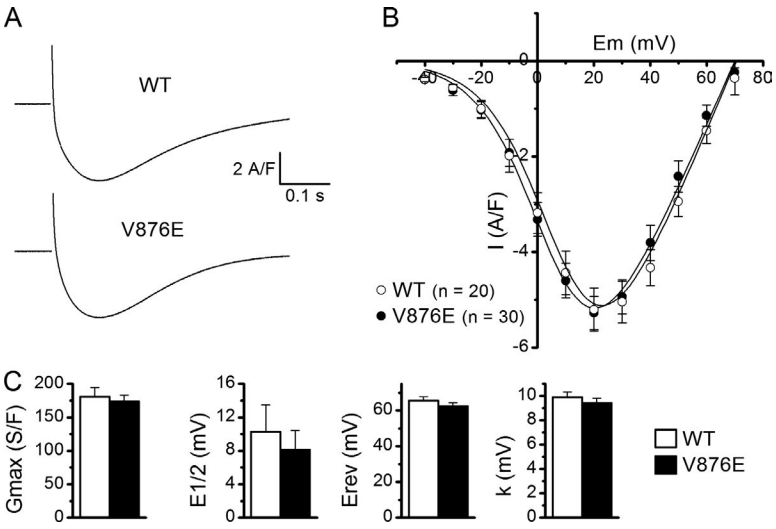

Figure 2. **L-type voltage-gated Ca^{2+} currents in WT and V876E fibers.** (A) Recordings of L-type currents (top) in a WT and in a V876E fiber in response to depolarizing pulses of 1 s duration to the indicated voltages (bottom). (B) Relationships between the mean peak values of L-type Ca^{2+} currents and membrane voltage in the two fiber types. (C) Mean of the fitting parameters of current-voltage relationships obtained in each WT and V876E fiber. E1/2, half-activation voltage; Erev, apparent reversal potential; Gmax, maximum conductance; k, steepness factor. Data are given as means ± SEM.

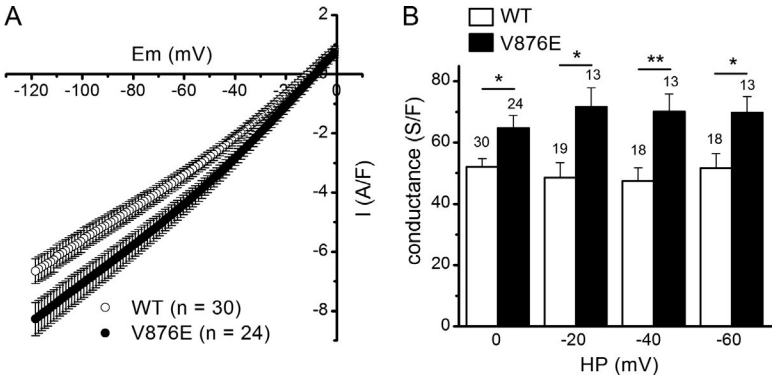

Figure 3. **Leak currents and leak conductance in WT and V876E fibers.** (A) Means and SEM of current densities evoked by voltage ramps applied from a holding potential of 0 mV in WT and R1239H fibers. The number of data points has been reduced for clarity. (B) Mean slope membrane conductance measured between −120 and −80 mV for voltage ramp–evoked membrane currents in the two fiber types from different holding potentials (HP). The number of fibers tested is indicated above each histogram bar. The p-values were 0.009, 0.006, 0.003, and 0.017 at 0, −20, −40, and −60 mV, respectively. Data are given as means ± SEM. *, $P < 0.05$; **, $P < 0.005$.

cell the current obtained at pH 7.2 from the current obtained at pH 6.0 revealed a current displaying an inward rectification and of significantly higher amplitude at −80 mV in V876E (−0.95 ± 0.14 A/F) as compared with WT fibers (-0.36 ± 0.19 A/F, P = 0.015), suggesting that the elevated leak current in V876E fibers is carried at least in part by H^+ (Fig. 4 B).

Acid-induced changes in pHi in V876E fibers in the presence of an external physiological solution

To determine whether the elevated leak current in V876E fibers is still carried by H^+ in the presence of a physiological saline, we measured the rate of intracellular acidification induced by a decrease of the external pH from 7.2 to 5 in a comparative manner in WT and V876E fibers, assuming that if the elevated leak current is actually carried by H^+, the rate of intracellular acidification arising from H^+ influx should be higher in V876E fibers. Fig. 5 A shows that the pHi monitored by the fluorescent pH indicator BCECF decreased in a reversible manner in response to a decrease of external pH from 7.2 to 5 at −80 mV, giving evidence of an influx of H^+ into the cell. Fitting a linear regression to the rate of change in pHi in all V876E and WT fibers showed that the rate of influx of H^+ was not significantly different in the two fiber types (Fig. 5, B and C). This result suggests that in the presence of an external solution containing Na^+ and K^+ monovalent cations, the elevated leak current in V876E is not associated with an increased influx of H^+ and in this way is certainly not carried by H^+. Interestingly, during the course of these experiments performed in the presence of an external Tyrode's solution, we noticed that there was a tendency for the mean background current at −80 mV to be more negative in V876E (−9.9 ± 3 A/F) than in WT fibers (−4.3 ± 0.8 A/F, P = 0.06). Because Na^+ is the only monovalent cation the electrochemical gradient of which is in favor of an influx at −80 mV, this observation led us to hypothesize that the cation carried by the elevated inward resting current in V876E fibers is Na^+.

Measurement of Na^+ influx at negative voltages in WT and V876E fibers

To investigate whether the elevated leak current in V876E carries Na^+, we measured the rate of increase in intracellular Na^+ arising from the replacement of an external solution containing 140 mM of the nonpermeant ion NMDG and devoid of Na^+ with a solution containing 140 mM Na^+ using the fluorescent Na^+ indicator SBFI. Fig. 6 A shows that such a change in the Na^+ concentration produced a reversible increase in the fluorescence ratio of SBFI associated with the development of an inward current and an increase in the membrane conductance at −80 mV in a V876E fiber. This result indicates that an open ion pathway allows a Na^+ influx to occur at rest in response to substitution of Na^+ for NMDG in the external solution. This effect was also observed in WT fibers but, on average, the rate of Na^+ influx was significantly larger in V876E fibers as compared with WT fibers (Fig. 6, B and C). A significant higher rate of Na^+ influx was also measured in V876E

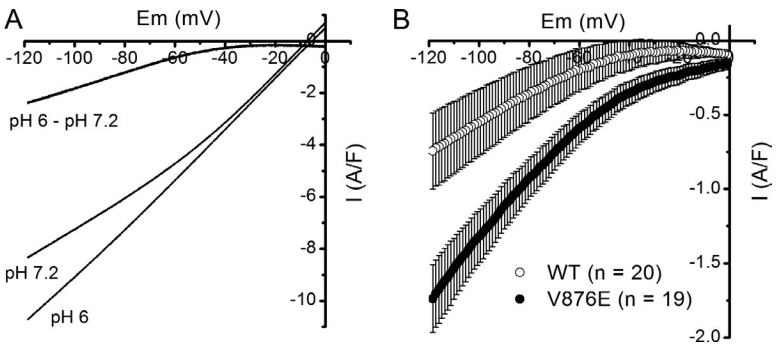

Figure 4. **Effect of external acidification on leak currents in WT and V876E fibers.** (A) Membrane currents evoked by a voltage ramp applied from a holding potential of 0 mV at an external pH of 7.2 and 6, and current difference between pH 6.0 and 7.2 in the same V876E fiber. (B) Means and SEM of current differences between pH 6.0 and pH 7.2 in WT and V876E fibers. The number of data points has been reduced for clarity.

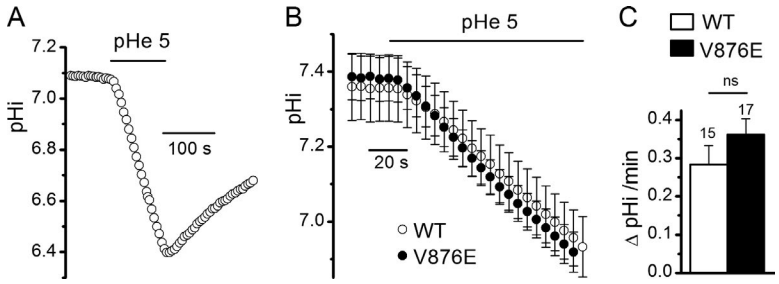

Figure 5. **Effect of external acidification on pHi in WT and V876E fibers in the presence of an external Tyrode's solution.** (A) Recording of the change in pHi in response to exposition of the cell to an external solution buffered at pH 5.0 in a BCECF-loaded V876E fiber held at −80 mV. (B) Means and SEM of pHi as a function of time in WT and in V876E fibers in response to external acidification (pHe). (C) Mean rate of change in pHi measured during the first minute of exposition of the cell to the external solution buffered at pH 5. The number of fibers tested is indicated above each histogram bar. Data are given as means ± SEM.

fibers when Tris instead of NMDG was used as the Na^+ substitute (not depicted).

Changes in background current induced by substitution of external Na^+ for NMDG in WT and V876E fibers

As expected from the preceding set of experiments, measurement of the background current at −80 mV in each WT and V876E fiber indicated that the mean current in the two fiber types was very significantly more inward when Na^+ ions were present in the external solution than when they were absent (Fig. 7 A). However, whereas the amplitude of the resting current was not significantly different in V876E and in WT fibers in the absence of external Na^+, it was significantly larger in V876E fibers when Na^+ was present in the external solution. This suggests that V876E fibers exhibit a higher leak sodium current at rest as compared with WT fibers. To confirm this higher Na^+ resting conductance in V876E fibers, fibers were challenged by hyperpolarizing voltage ramps in the presence and in the absence of external Na^+. As expected, the background current was considerably more inward and the slope conductance larger when Na^+ was substituted for NMDG in V876E fibers (Fig. 7 B). This effect was also observed in WT fibers but, on average, the slope conductance measured between −110 and −80 mV in the presence of external Na^+ was significantly larger in V876E (273 ± 23 S/F) than in WT fibers (205 ± 23 S/F, P = 0.049; Fig. 7 C).

DISCUSSION

The valine residue at position 876 in the α1 subunit of the voltage-dependent Ca^{2+} channel is highly conserved not only among channel proteins from various species but also among different α1 subunits (Ke et al., 2009). Amino acid substitution at this location is thus expected to induce critical channel dysfunctions, possibly pathogenic. Nevertheless, in transfecting the genes encoding the human WT and the HypoPP1 V876E mutant α1 subunits in adult mice muscles, we showed that the properties of the voltage-gated Ca^{2+} currents are not altered by the mutation. These data differ from the functional results obtained with the other R528H HypoPP1 and R1239H mutations so far investigated, for which the maximal conductance and voltage dependence of the voltage-gated Ca^{2+} currents were found to be altered (Lapie et al., 1996; Jurkat-Rott et al., 1998; Morrill et al., 1998; Wu et al., 2012; Fuster et al., 2017). Concerning these mutations, it has been recurrently claimed that the observed changes in the Ca^{2+} channel properties

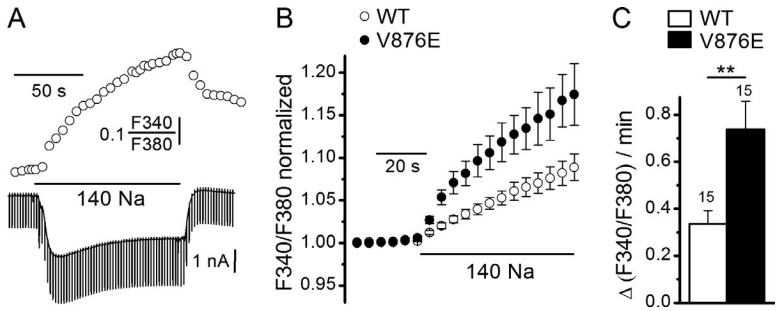

Figure 6. **Effect of external Na^+ on SBFI fluorescence ratio and background currents in WT and V876E fibers.** (A) Simultaneous recordings of SBFI fluorescence ratio (upper trace) and membrane currents (lower trace) in response to a change of the external solution from a Na^+-free NMDG containing solution to a 140 mM Na^+–containing solution in a V876E fiber held at −80 mV and stimulated by 50-ms duration voltage pulses given to −90 mV at a frequency of 0.5 Hz. (B) Mean and SEM of SBFI fluorescence ratio as a function of time in response to external Na^+ readmission in WT and in V876E fibers. In each cell, values of fluorescence ratio have been normalized to the value of the last data point measured before Na^+ readmission. (C) Mean rate of change in SBFI fluorescence ratio measured during the first 30 s of exposure of the cell to external Na^+. The number of fibers tested is indicated above each histogram bar. Data are given as means ± SEM. P-value was 0.0043 (**).

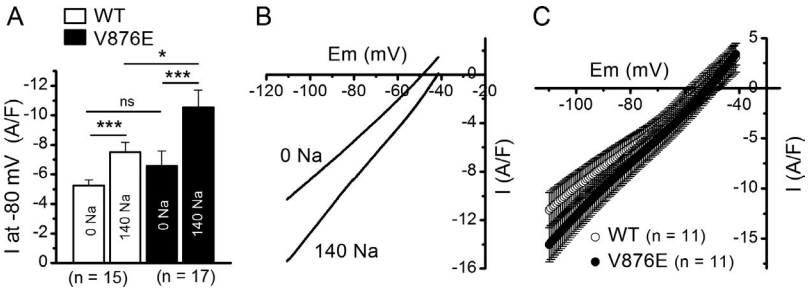

Figure 7. **Effect of external Na^+ on leak currents and conductance in WT and V876E fibers.** (A) Mean background current intensity measured at −80 mV in the absence and in the presence of external Na^+ in WT and V876E fibers. Values were compared with paired tests and unpaired tests for data obtained within the same fiber population and for data obtained between the two fiber populations, respectively. P-values were 0.0001 and 0.0001 for comparison of the means between the Na^+-free and the Na^+ containing solution in WT and V876E fibers, respectively, and 0.047 for comparison of the means obtained in the presence of the Na^+–containing solution in WT and V876E fibers. Data are given as means ± SEM. *, $P < 0.05$; ***, $P < 0.0005$. (B) Membrane currents evoked by a voltage ramp applied from a holding potential of −40 mV in the absence and in the presence of external Na^+ in the same V876E fiber. (C) Means and SEM of current densities evoked by voltage ramps applied from a holding potential of −40 mV in the presence of external Na^+ in WT fibers and V876E fibers. The number of data points has been reduced for clarity.

could hardly explain the pathogenesis of HypoPP1. The fact that the V876E mutation induced HypoPP1 without changing the properties of the voltage-gated Ca^{2+} channel here demonstrates and confirms that the HypoPP1 pathogenesis is not related to any change in the Ca^{2+} channel function of Cav1.1 and also suggests that the global voltage sensing function of domain III, which has been shown to be directly involved in channel activation, is not altered (Pantazis et al., 2014).

The main finding of our study is that fibers expressing the V876E mutation exhibited a larger leak inward current over a range of voltages negative to −40 mV as compared with fibers expressing WT Cav1.1. Such an elevated inward current at resting potentials has been detected in R528H and in R1239H muscle fibers (Jurkat-Rott et al., 2009; Wu et al., 2012; Fuster et al., 2017). Because these HypoPP1 mutations correspond to the replacement of the first or the second outermost arginine with a histidine in the S4 segment of domain II or domain IV, respectively, it has been postulated that the observed leak current flowed through a gating pore generated by the mutation as has been observed for similar mutations in voltage-gated K^+ or Na^+ channels (Starace and Bezanilla, 2004; Sokolov et al., 2005; Tombola et al., 2005). In WT channels, S4 segments are indeed thought to translocate across a "gating pore" pathway formed by the S1, S2, and S3 segments through interactions between arginine residues in S4 segments and negatively charged residues in the three other segments. The loss of interaction produced by arginine mutation to uncharged residues has been shown to make the gating pore permeable to H^+ or monovalent cations generating a gating pore current at negative voltages when the mutation affects the outermost arginine in the S4 segment (Starace and Bezanilla, 2004; Struyk and Cannon, 2007). The V876E mutation does not directly affect an arginine residue in a S4 segment, but the fact that it produced an inward current at rest likely suggests that a gating pore able to pass monovalent cations at negative voltages has been created. Our data are thus reminiscent of histidine scanning mutagenesis studies in the Shaker K^+ channel, which showed that mutations not located in the S4 segment and consisting in the replacement of an isoleucine with a histidine in segment S2 created a gating pore by disrupting the hydrophobic barrier lined in part by isoleucine and the most extracellular arginine of the S4 segment (Campos et al., 2007). We thus hypothesize that V876 and one of the most extracellular charged residues in the S4 segment are also part of a narrow hydrophobic plug separating the water-accessible crevices on each side of the membrane that disrupts and allows bridging of the internal and external solutions through a gating pore when valine is replaced by glutamate, in the same manner as the gating pore created by arginine substitution in S4 segments. This local hydrophilic shortcut could be produced by modification in the electrostatic interactions with the positively charged residues of the S4 segment because of the presence of the negatively charged residue glutamate or alternatively by widening the gating pore entrance through structural displacement of the S3 segment. The structural perturbations created by this valine-to-glutamate mutation do not seem to affect the global structure and function of the voltage-sensing domain of domain III because the biophysical properties of the channels were found to remain unchanged. Therefore, the V876E mutation is to our knowledge the first mutation located in an S3 segment giving rise to an elevated leak current at negative voltages, possibly flowing through a gating pore, without any change in the basic voltage-dependent channel properties.

The extra leak current induced by the V876E mutation displayed an apparent inward rectification when recorded in the absence of external permeant monovalent cations (Figs. 3 A and 4 A). Such a rectification was also evident for the extra leak current recorded by Wu et al. (2012) in the Cav1.1 R528H transgenic mouse in the absence of external permeant ions and for the

leak current recorded in muscle fibers from R528H and R1239H patients by Jurkat-Rott et al. (2009) in the presence of 1 mM external K^+, which should considerably reduce the contribution of the inward rectifier K^+ current, and in fibers expressing the R1239H channel mutant (Fuster et al., 2017). This inward rectification is reminiscent of the rectification originally observed in the *Shaker* K^+ channel for mutations affecting the outermost arginine and demonstrated to be imposed by a voltage-dependent mechanism that closes the pore at positive potentials (Starace and Bezanilla, 2004). Interestingly, inward rectification was also reported for the gating pore generated by mutation in the S2 segment, indicating that the outward movement of the S4 segment in response to depolarization also led to the closure of this S2 mutant-induced gating pore (Campos et al., 2007). Therefore, if the extra inward leak current recorded in V876E fibers does indeed represent permeation through a gating pore, its voltage dependence of activation should correlate with the voltage dependence of movement of the S4 voltage sensor. Figs. 3 A and 4 A indicate that the extra current develops for potentials lower than −50 mV and progressively abrogates at higher voltages. In skeletal muscle, the movement of S4 voltage sensors gives rise to intramembrane charge movements with a reported half activation of −37 mV in mouse skeletal muscle (Collet et al., 2003). The voltage dependence of activation of charge movements thus matches well with the voltage-dependent reduction of the extra current in mutant fibers, which again argues in favor of this current flowing through a gating pore gated by the voltage-driven movement of S4 segments. Additionally, the observed inward rectification of the extra current in V876E fibers excludes that this current may have flowed through the L-type Ca^{2+}-conducting pore of the channel because it develops at voltages much more negative than the voltage threshold of the L-type current and moreover from a holding potential of 0 mV, for which the L-type current is inactivated.

Our experiments performed in the absence of external permeant monovalent cations showed that the resting inward leak current was potentiated by external acidification in V876E, suggesting that it can be carried, at least in part, by H^+, as demonstrated for the R1239H mutation (Fuster et al., 2017). But, in contrast to what has been found for the R1239H mutation, the fact that the rate of H^+ influx in response to external acidification in the presence of an external Tyrode's solution was not different in WT and V876E fibers led us to conclude that this V876E-induced current was not carried by H^+ when Na^+ and K^+ ions are present in the external solution and used a pathway with different ion selectivity as compared with the pathway used in R1239H fibers. Indeed, changing the external solution from a Na^+-free to a Na^+-containing solution at resting potentials was found to produce an influx of Na^+ associated with an inward current in WT and in V876E fibers. A Na^+ influx is known to occur in resting muscle (Hodgkin and Horowicz, 1959), but our experiments indicate that this influx and the associated inward current are significantly larger in V876E fibers. These data strongly suggest that the extra current in V876E fibers mainly carries Na^+. In agreement with these findings, site-directed mutagenesis studies of the voltage-gated Na^+ channel have shown that the gating pore is selective to H^+ when the gating pore results from the replacement of an arginine with a histidine, whereas it passes Na^+ or K^+ when residues other than histidine are substituted for arginine (Starace and Bezanilla, 2004; Tombola et al., 2005; Sokolov et al., 2007; Struyk and Cannon, 2007). Nevertheless, our experiments indicate that in the absence of Na^+ and K^+, the V876E-induced leak current is able to carry H^+. In the Na^+-free Tyrode's solution, we postulate that the high resting K^+ conductance may mask the elevated H^+ current that should flow through the mutation-induced pathway, explaining in this way why the leak current is not different between WT and V876E fibers under these Na^+-free conditions.

Challenging fibers with voltage ramps indicated that the leak conductance was, on average, 205 and 273 S/F in WT and in V876E fibers, respectively. If we assume that the difference in leak conductance is entirely a result of the presence of a Na^+ gating pore current, this indicates that the mean conductance of the gating pore is 68 S/F. As compared with the leak conductance measured in muscle fibers from HypoPP1 R528H transgenic mice, HypoPP1 patients' muscle biopsies, or R12639H mutant-expressing fibers (Jurkat-Rott et al., 2009; Wu et al., 2012; Fuster et al., 2017), the leak conductance induced by the HypoPP1 V876E mutation is at least 3 times larger and certainly even more if we consider that not all native Cav1.1 have been replaced by the transfected channels. Such a large resting leak current has to be related to the high severity of the symptoms reported for this form of HypoPP1. This mutation was indeed identified in a South American family with an uncommon early age of onset of the disease, high penetrance, and very severe prognosis (Ke et al., 2009). Attacks of paralysis are thought to be triggered by a sudden depolarization of muscle cells inducing inactivation of voltage-gated Na^+ channels. In skeletal muscle, the resting potential is setting up at a value for which depolarizing inward currents are exactly balanced by hyperpolarizing outward currents. The conditions that lead to an inbalance between inward and outward currents and the resulting depolarization in HypoPP1 are still matters of debate. It is, however, indisputable that our finding of a high Na^+ leak current in V876E has very important pathophysiological consequences because the higher the depolarizing inward current, the higher the expected depolarization of resting potential and severity of the symptoms.

In conclusion, the first functional characterization of the V876E HypoPP1 mutation demonstrates the existence of a hydrophilic pathway possibly corresponding to a gating pore in the voltage sensor domain of the voltage-gated Ca^{2+} channel that generates Na^+ current at resting membrane potentials. Our data thus may suggest that the generation of a gating pore constitutes a pathogenic mechanism common to all HypoPP1 disorders, the severity of which may be related to the intensity of the depolarizing current induced by the mutation.

ACKNOWLEDGMENTS

This study was supported by the University Lyon 1, the Centre National de la Recherche Scientifique, the Institut National de la Santé et de la Recherche Médicale, and the Association Française contre les Myopathies (AFM-Téléthon, grant 18241).

The authors declare no competing financial interests.

Author contributions: C. Fuster designed and performed experiments and analyzed data. J. Perrot performed experiments. C. Berthier designed and performed experiments. V. Jacquemond gave conceptual advice. P. Charnet gave conceptual advice and wrote the paper. B. Allard designed and performed experiments, analyzed data, and wrote the paper.

Eduardo Ríos served as editor.

Submitted: 16 June 2017
Revised: 18 September 2017
Accepted: 12 October 2017

REFERENCES

Campos, F.V., B. Chanda, B. Roux, and F. Bezanilla. 2007. Two atomic constraints unambiguously position the S4 segment relative to S1 and S2 segments in the closed state of Shaker K channel. *Proc. Natl. Acad. Sci. USA.* 104:7904–7909. https://doi.org/10.1073/pnas.0702638104

Cannon, S.C. 2010. Voltage-sensor mutations in channelopathies of skeletal muscle. *J. Physiol.* 588:1887–1895. https://doi.org/10.1113/jphysiol.2010.186874

Cannon, S.C. 2015. Channelopathies of skeletal muscle excitability. *Compr. Physiol.* 5:761–790. https://doi.org/10.1002/cphy.c140062

Catterall, W.A. 2011. Voltage-gated calcium channels. *Cold Spring Harb. Perspect. Biol.* 3:a003947. https://doi.org/10.1101/cshperspect.a003947

Collet, C., L. Csernoch, and V. Jacquemond. 2003. Intramembrane charge movement and L-type calcium current in skeletal muscle fibers isolated from control and *mdx* mice. *Biophys. J.* 84:251–265. https://doi.org/10.1016/S0006-3495(03)74846-2

DiFranco, M., P. Neco, J. Capote, P. Meera, and J.L. Vergara. 2006. Quantitative evaluation of mammalian skeletal muscle as a heterologous protein expression system. *Protein Expr. Purif.* 47:281–288. https://doi.org/10.1016/j.pep.2005.10.018

Fuster, C., J. Perrot, C. Berthier, V. Jacquemond, and B. Allard. 2017. Elevated resting H(+) current in the R1239H type 1 hypokalaemic periodic paralysis mutated Ca(2+) channel. *J. Physiol.* 595:6417–6428. https://doi.org/10.1113/JP274638

Gandhi, C.S., and E.Y. Isacoff. 2002. Molecular models of voltage sensing. *J. Gen. Physiol.* 120:455–463. https://doi.org/10.1085/jgp.20028678

Hodgkin, A.L., and P. Horowicz. 1959. Movements of Na and K in single muscle fibres. *J. Physiol.* 145:405–432. https://doi.org/10.1113/jphysiol.1959.sp006150

Jurkat-Rott, K., U. Uetz, U. Pika-Hartlaub, J. Powell, B. Fontaine, W. Melzer, and F. Lehmann-Horn. 1998. Calcium currents and transients of native and heterologously expressed mutant skeletal muscle DHP receptor α1 subunits (R528H). *FEBS Lett.* 423:198–204. https://doi.org/10.1016/S0014-5793(98)00090-8

Jurkat-Rott, K., M.A. Weber, M. Fauler, X.H. Guo, B.D. Holzherr, A. Paczulla, N. Nordsborg, W. Joechle, and F. Lehmann-Horn. 2009. K^+-dependent paradoxical membrane depolarization and Na^+ overload, major and reversible contributors to weakness by ion channel leaks. *Proc. Natl. Acad. Sci. USA.* 106:4036–4041. https://doi.org/10.1073/pnas.0811277106

Jurkat-Rott, K., J. Groome, and F. Lehmann-Horn. 2012. Pathophysiological role of omega pore current in channelopathies. *Front. Pharmacol.* 3:112. https://doi.org/10.3389/fphar.2012.00112

Ke, T., C.R. Gomez, H.E. Mateus, J.A. Castano, and Q.K. Wang. 2009. Novel CACNA1S mutation causes autosomal dominant hypokalemic periodic paralysis in a South American family. *J. Hum. Genet.* 54:660–664. https://doi.org/10.1038/jhg.2009.92

Lapie, P., C. Goudet, J. Nargeot, B. Fontaine, and P. Lory. 1996. Electrophysiological properties of the hypokalaemic periodic paralysis mutation (R528H) of the skeletal muscle alpha 1s subunit as expressed in mouse L cells. *FEBS Lett.* 382:244–248. https://doi.org/10.1016/0014-5793(96)00173-1

Lehmann-Horn, F., R. Rüdel, and K. Jurkat-Rott. 2004. Nondystrophic myotonias and periodic paralyses. *In* Myology. Third edition. McGraw-Hill, New York. 1257–1300.

Matthews, E., and M.G. Hanna. 2010. Muscle channelopathies: does the predicted channel gating pore offer new treatment insights for hypokalaemic periodic paralysis? *J. Physiol.* 588:1879–1886. https://doi.org/10.1113/jphysiol.2009.186627

Melzer, W., A. Herrmann-Frank, and H.C. Lüttgau. 1995. The role of Ca^{2+} ions in excitation-contraction coupling of skeletal muscle fibres. *Biochim. Biophys. Acta.* 1241:59–116. https://doi.org/10.1016/0304-4157(94)00014-5

Moreau, A., P. Gosselin-Badaroudine, and M. Chahine. 2014. Biophysics, pathophysiology, and pharmacology of ion channel gating pores. *Front. Pharmacol.* 5:53. https://doi.org/10.3389/fphar.2014.00053

Morrill, J.A., R.H. Brown Jr., and S.C. Cannon. 1998. Gating of the L-type Ca channel in human skeletal myotubes: an activation defect caused by the hypokalemic periodic paralysis mutation R528H. *J. Neurosci.* 18:10320–10334.

Pantazis, A., N. Savalli, D. Sigg, A. Neely, and R. Olcese. 2014. Functional heterogeneity of the four voltage sensors of a human L-type calcium channel. *Proc. Natl. Acad. Sci. USA.* 111:18381–18386. https://doi.org/10.1073/pnas.1411127112

Ríos, E., and G. Pizarro. 1991. Voltage sensor of excitation-contraction coupling in skeletal muscle. *Physiol. Rev.* 71:849–908.

Robin, G., and B. Allard. 2015. Voltage-gated Ca^{2+} influx through L-type channels contributes to sarcoplasmic reticulum Ca^{2+} loading in skeletal muscle. *J. Physiol.* 593:4781–4797. https://doi.org/10.1113/JP270252

Schneider, M.F. 1994. Control of calcium release in functioning skeletal muscle fibers. *Annu. Rev. Physiol.* 56:463–484. https://doi.org/10.1146/annurev.ph.56.030194.002335

Sokolov, S., T. Scheuer, and W.A. Catterall. 2005. Ion permeation through a voltage-sensitive gating pore in brain sodium channels having voltage sensor mutations. *Neuron.* 47:183–189. https://doi.org/10.1016/j.neuron.2005.06.012

Sokolov, S., T. Scheuer, and W.A. Catterall. 2007. Gating pore current in an inherited ion channelopathy. *Nature.* 446:76–78. https://doi.org/10.1038/nature05598

Starace, D.M., and F. Bezanilla. 2004. A proton pore in a potassium channel voltage sensor reveals a focused electric field. *Nature.* 427:548–553. https://doi.org/10.1038/nature02270

Struyk, A.F., and S.C. Cannon. 2007. A Na^+ channel mutation linked to hypokalemic periodic paralysis exposes a proton-selective gating pore. *J. Gen. Physiol.* 130:11–20. https://doi.org/10.1085/jgp.200709755

Tombola, F., M.M. Pathak, and E.Y. Isacoff. 2005. Voltage-sensing arginines in a potassium channel permeate and occlude cation-selective pores. *Neuron.* 45:379–388. https://doi.org/10.1016/j.neuron.2004.12.047

Wu, F., W. Mi, E.O. Hernández-Ochoa, D.K. Burns, Y. Fu, H.F. Gray, A.F. Struyk, M.F. Schneider, and S.C. Cannon. 2012. A calcium channel mutant mouse model of hypokalemic periodic paralysis. *J. Clin. Invest.* 122:4580–4591. https://doi.org/10.1172/JCI66091